Fuzzy control mathematical modelling method based on dynamic particle swarm optimisation training

Runxia Gao* and Houping Jiang

Anqing Vocational and Technical College,
Anqing Anhui, 246003, China
Email: 2829289221@qq.com
Email: 171385646@qq.com
*Corresponding author

Abstract: Aiming at the false correlation problems under set number limit condition in the fuzzy control mathematic modelling process, combined with dynamic particle swarm optimisation training algorithm, the traditional fuzzy control mathematical model based on the Nash equilibrium solution method is difficult to converge to the optimal solution of the state space, leading to bad control performance. This paper proposes the fuzzy control mathematical modelling method based on dynamic particle swarm optimisation training, constructs the general structure model of fuzzy control, describes the standard particle algorithm under the constraint of learning samples of random functional, obtains the global optimal solution of control domain of fuzzy control parameters, and conducts particle swarm optimisation training by adopting the position vector fitness updating method. The research results show that the new method can make every step state update get more effective observation information, reduce the error caused by the difficult use of observation data, reduce the computation cost and improve the accuracy of fuzzy control.

Keywords: fuzzy control; observation error; ensemble transform Kalman filter; ETKF.

Reference to this paper should be made as follows: Gao, R. and Jiang, H. (2021) 'Fuzzy control mathematical modelling method based on dynamic particle swarm optimisation training', *Int. J. Innovative Computing and Applications*, Vol. 12, No. 1, pp.48–55.

Biographical notes: Runxia Gao received her Master's in Mathematics from Anhui University. Her research interests include applied mathematics and higher vocational mathematics education.

Houping Jiang received his Master's in Business Administration from University of Science and Technology of China. His research interests include economic management and business management.

1 Introduction

In the studies of atmosphere, ocean, geophysics and nonlinear dynamical systems, fuzzy control refers, in the evolution process of dynamical models, continuously integrating the new observation information, obtaining the best estimate of the current state, improving the model prediction precision and reducing the uncertainty, and describing the true state of the atmosphere, ocean, and land surface as accurately as possible (Chang and Yang, 2010; Chen et al., 2010; Li et al., 2009). In the process of fuzzy control, it is not feasible to measure the global system state directly, and the observation frequency is usually far lower than the model evolution frequency. We must select suitable observation data to estimate the state of Li et al. (2009), Mora-Gutiérrez et al. (2016), Hu et al. (2010) and Kalyoncu and Haydim (2009). At the same time, the nonlinear state of the model is relatively complex, and if it is not able to provide effective observation data, the state estimation is deviated from the real state (Lin, 2012; Lima et al., 2010; Vembarasan and Balasubramaniam, 2013; Faria et al., 2013). Therefore, how to use the observation data reasonably and improve the accuracy of the forecast is a hot research issue in recent years. Based on the consistency analysis criterion, the statistical observation value minus the analysis value is relied on to replace the observation error statistics (Crawford et al., 2013; Gandomi et al., 2013; Roberge et al., 2013; Maldonado et al., 2013). By taking the average value of the observation data in a certain region, reduce the observation random error and the relevant error so to reduce the risk of the smooth atmospheric characteristics (Palafox et al., 2013; Lian et al., 2014; Mohammadi-Ivatloo et al., 2013; Ghamisi et al., 2014). Since the observation error covariance matrix of has the form similar to the symmetric Toeplitz circulation matrix, make discrete Fourier transform (DFT) of this circulation matrix to more accurately estimate the observation error covariance matrix (Kalyoncu and Haydim, 2009; Lin, 2012). The result of the target observation based on the maximum set variance shows that the state estimation is better than the local ensemble transform Kalman filter (ETKF) method (Helwig et al., 2013; Marinakis et al., 2013). However, in actual assimilation, the more accurate expression of state estimation is mainly dependent on the real-time updating of observation information. How to get more accurate and effective observation information and reduce the analysis error caused by the difficult use of observation data is worth further studying (Formisano et al., 2013). In the traditional methods, the mathematical modelling methods for the fuzzy control mainly include the control system mathematical modelling method based on the game model, the fuzzy control mathematical modelling method based on the particle swarm algorithm, the fuzzy control mathematical modelling method based on the neural network and so on (Sinha et al., 2013). The variable multi-component input method is adopted by such type of methods to carry out the precise control of the system and improve the effectiveness and accuracy of the mathematical modelling. However, due to the uncertainty of the components, the control system is prone to divergence (Ting et al., 2014). The application of the Nash equilibrium method makes it difficult to converge to the optimal solution in the state space, resulting in poor control performance.

This paper proposes a fuzzy control mathematical modelling method based on particle swarm optimisation (PSO) training. It firstly constructs the overall structure model of the fuzzy control, conducts the standard particle algorithm description, based on the standard particle swarm algorithm adopts the position vector fitness update method for PSO training, then introduces the fuzzy controller design, constructs the observation position equivalent weights, and state estimation analytical expressions; finally, it verifies the new method, compares with the traditional method, and discusses the effectiveness of the algorithm.

2 Fuzzy control parametric model and standard particle swarm description

2.1 Fuzzy control parametric model

In order to implement the mathematical modelling of the fuzzy control system, it is necessary to carry out the fuzzy control parametric model analysis. In the construction of the parametric model, the given fuzzy control is a kind of nonlinear control. The basic idea of the fuzzy mathematics is used to describe the system variable structure and the parametric model correctly. It is assumed that the structural model description of a fuzzy control system is shown in Figure 1.

Figure 1 Structure model of the fuzzy control system

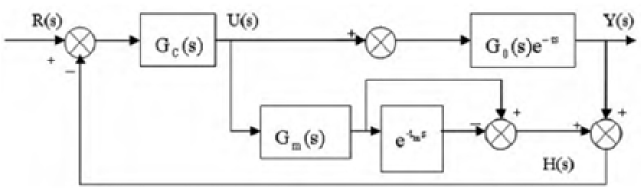

In the control system shown in Figure 1, the input to the controller is as the following:

$$\begin{pmatrix} X \\ P(X) \end{pmatrix} = \begin{Bmatrix} a_1, a_2, ..., a_m \\ p(a_1), p(a_2), ..., p(a_m) \end{Bmatrix} \tag{1}$$

In which, $0 \le p(a_i) \le 1$ ($i = 0, 1, 2, \cdots, m$) stands for the time delay function of the fuzzy control. When the above-mentioned control process is given in the form of discrete sampling, the closed-loop system of the intelligent fuzzy control is constructed as the following:

$$\dot{x}(t) = Ax(t) + BKx\left(t - d_s(t) - d_a(t)\right) \tag{2}$$

When the weight at each layer is not correlated with the skew vector $G_m(s) = G_0(s)$, $t_m = \tau$, and the feedback control signal can be obtained as the following:

$$H(s) + Y(s) = G_m(s)U(s) \tag{3}$$

The entropy of functional information of the feedback control mathematical model is as the following:

$$H(X) = E\left(I(a_i)\right) = -\sum_{i=1}^{m} p(a_i) \log_2 p(a_i) \tag{4}$$

Under the constraints of the stochastic functional learning samples and the system reaches the equilibrium, the characteristic equation of the fuzzy control system carries out the complete tracking compensation for the fuzzy immune time delay link to obtain the following.

$$\begin{aligned} &\frac{Y(s)}{R(s)} \\ &= \frac{G_c(s)G_0(s)e^{-\tau s}}{1 + G_c(s)G_m(s) + G_c(s)\left(G_0(s)e^{-\tau s} - G_m(s)e^{-t_m s}\right)} \end{aligned} \tag{5}$$

In the fuzzy control parametric structure model, it is assumed that the control performance index function is as the following:

$$F(x) = E\left[\sum_{k=1}^{m} e_k^2\right] = E\left[e^T e\right] \tag{6}$$

In which e stands for the mean square error of the mean absolute error performance function, and e_k stands for its k^{th} component. Through the linear feedback control designed in this paper, the 7 degree of freedom Smith decomposition problem of the fuzzy control system is converted into the two degree of freedom control model to improve the control performance and the capability. And the fuzzy feedback linear control output thus obtained is as the following:

$$\frac{\partial F}{\partial o_k} = \frac{\partial F}{\partial y_k} \bullet \frac{\partial y_k}{\partial o_k} \tag{7}$$

$$\frac{\partial F}{\partial z_{kj}} = \frac{\partial F}{\partial o_k} \bullet \frac{\partial o_k}{\partial z_{kj}} \tag{8}$$

$$\frac{\partial F}{\partial w_{ji}} = \sum_{k=1}^{m} \frac{\partial F}{\partial o_k} \bullet \frac{\partial o_k}{\partial a_j} \bullet \frac{\partial a_j}{\partial net_j} \bullet \frac{\partial net_j}{\partial w_{ji}} \tag{9}$$

In which $x(t) = [x_1(t), x_2(t), \cdots, x_i(t)]^T$ stands for the state vector of the particles randomly selected at the time t, $d_1(t)$ and $d_2(t)$ stand for the probability characteristics of two wings, respectively. The $d(t) = d_1(t) + d_2(t)$ is defined to obtain the global optimal weight value of the fuzzy control system as the following:

$$\frac{Y(s)}{R(s)} = \frac{G_c(s)G_0(s)e^{-\tau s}}{1 + G_c(s)G_0(s)} \tag{10}$$

In the above equation, $G_c(s)$ and $G_0(s)$ stand for the number of evolving generations and the initial fitness value. The parametric model of the fuzzy control system constructed above is used as the mathematical basis to construct the mathematical model.

2.2 Standard particle swarm algorithm

In the fuzzy control parametric model constructed above, the standard particle swarm algorithm is adopted to train the parameters.

Assumption 1: Assume that the initial number of particles is N. For any Borel subset A of the control domain U of the fuzzy control parameter, where j = 1, 2, 3,... N, the following is met:

$$f(x_1) = f(x_2) = \cdots = f(x_n) = f^n \tag{11}$$

The initial fitness value of each particle is updated. When $s_i \in s^*$, the transition probability of the initial velocity and the position $\{A_k\}$ value of the particle swarm are the following:

$p_{ij}(k) = p\{A_{k+1}^j / A_k^i\} \geq 0$ is calculated, and the following can be obtained:

$$p_{ij}(k) = p\left\{A_{k+1}^j / A_k^i\right\} = \sum_{s_c \in S^2} p\left\{C_k^l / A_k^i\right\} \tag{12}$$

When $i \in I, j \notin I$ for any L, the particle training strategy in the feasible solution space is defined as the following:

$$p_i(t+1) = p_i(t) + \eta_1 \bullet \left(p_i(t) - p_j(t)\right) + \eta_2 Cauchy(\theta, \alpha) \tag{13}$$

In which, $Cauchy(\theta, \alpha)$ is standard Cauchy distribution, and the following can be obtained:

$$p\left\{A_{k+1}^j / A_k^i C_k^l\right\} = \sum_{s_c \in S^2} p\left\{C_k^l / A_k^i B_k^b\right\} \tag{14}$$

The standard particle swarm algorithm is adopted to carry out the fuzzy control training, according to the clone selection, the following is met:

$0 \leq \sigma_{ik} \leq 1, \sum_{k=1}^{K_i} \sigma_{ik} = 1,$ distribution $\sigma_i = (\sigma_{i1}, \cdots, \sigma_{iK_i})$, hence the probability can be obtained as the following:

$$p\left\{A_{k+1}^j / A_k^i B_k^b C_k^l\right\} = 0 \tag{15}$$

Simultaneous equations are set, and the following can be obtained: $p_{ij}(k) = 0$.

Lemma 1: It is assumed that the motion direction function f of the particle is a measurable function, and U is its own individual subset on R^n. In the process of fuzzy control, the Hypothesis 1 is met under $\{x_k\}_{k=0}^{+\infty}$, which is the solution sequence for each particle in the particle swarm. Hence $\lim_{t \to 0} P[x^k \in R_\varepsilon] = 1$ is established. The inertial weight of the j^{th} particle is ω, and R_ε stands for the set of the global optimal points.

Figure 2 Basic PSO algorithm flow

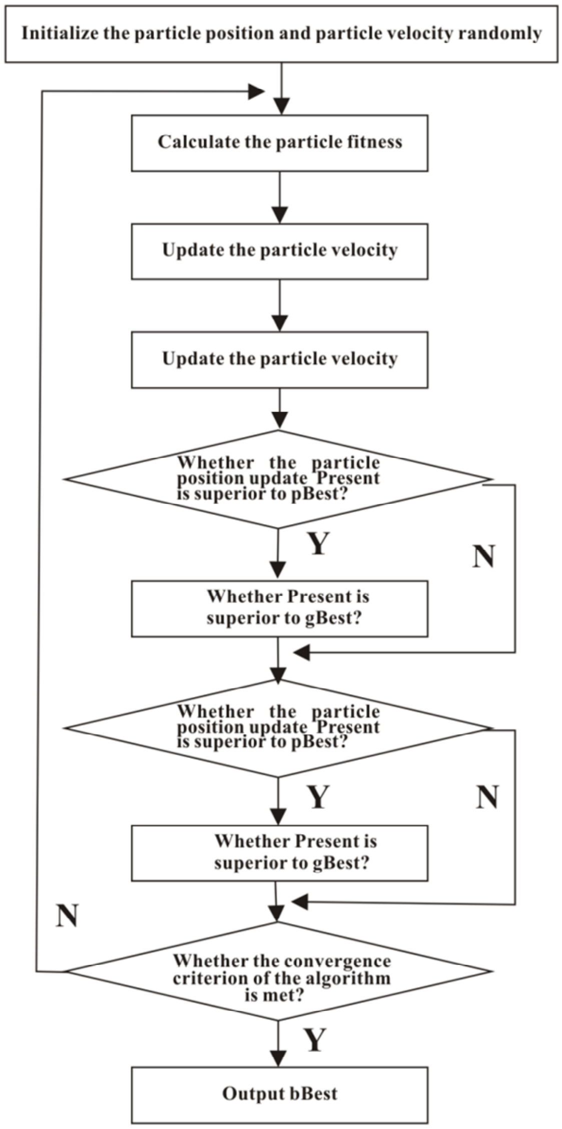

Theorem 1: It is assumed that the population size is m, the objective function f is a measurable function, and each parameter meets the following equation: $X_{g,k}$ stands for the search space vector of the k^{th} particle swarm. And $P[x_{g,k} \in R_\varepsilon]$ stands for the optimal solution obtained for the probability of $x_{g,k} \in R_\varepsilon$ in the state space in accordance with the standard particle swarm algorithm.

And the flow of the basic PSO algorithm is shown in Figure 2.

In general, the termination condition is set to a sufficiently good fitness value or to a preset maximum number of iterations. In addition, in accordance with the specific optimisation problem, it is necessary to limit the flight range and the maximum velocity of the particle. In addition, different ranges can be set for each dimension. During the process of the algorithm operation, the individual extremum of the particle and the global extremum of the particle swarm are updated continuously. At the end of the operation of the algorithm, the global extremum best shall be output.

3 Fuzzy control mathematical modelling process

This article takes ensemble transform Kalman conversion filter (ETKF) as the basis of the algorithm, in the assimilation process at the state update moment calculates and gets the Euclidean distance with the observation points, through the fuzzy theory conducts distance (physical space grid) judgment for the observation position, and gives the corresponding fuzzy weights. Therefore, it can effectively use observation data to reduce state estimation error, and to a certain extent avoid false correlation caused by too small set number so to make the prediction value more real and effective.

3.1 Introduction to fuzzy control principle

The fuzzy control system has strong robustness so to greatly weaken the influence of disturbance and parameter changes on control effect, especially for strong nonlinear and unstable situations in dynamic prediction mode. The observation weight in the assimilation system determines the importance of observation information at different observation points and the way of information expansion between observation space and different variables. Figure 3 gives a sketch map of the fuzzy control assimilation, in which the 'seven corner star' is the state updating position, and the 'pentagram' is the observation position. The traditional local assimilation scheme is based on sequential filtering. At the central lattice point of the localised area (the square area in Figure 3) through state variables and all observation data make successive circulation and evolution to all the analysis grids. Each analysis grid is independent of each other. Before the state estimation updating, the new method firstly calculates the Euclidean distance between the state update point and all observation points; then through fuzzy control makes fuzzy quantifying of the distance between the state update position and the observation position, and determines the weight of the observation point. The closer the distance to the state update position, the greater the weight of the observation value, and vice versa.

Figure 3 The sketch map of the dynamic PSO training

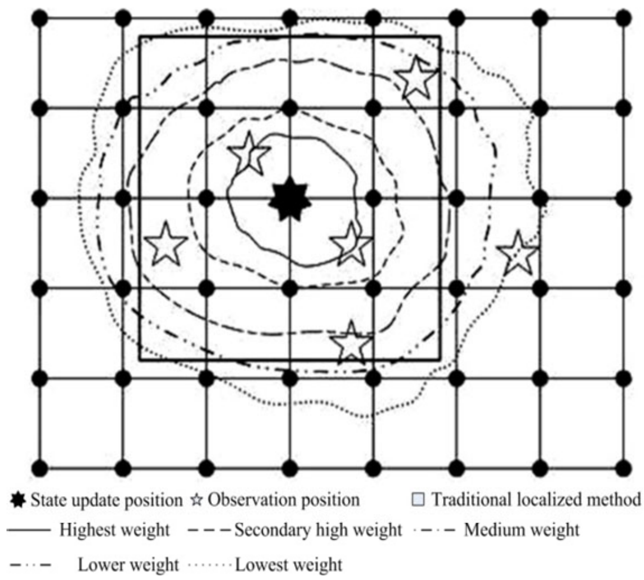

3.2 Dynamic PSO training

Through the dynamic PSO training obtain the weight of each observation point, and then calculate the state updating vector. The specific scheme process is as follows:

1 The selection and discretisation of the transformer's variation. According to the change of the Euclidean distance l between the observation position and the state update lattice point, take the linguistic variable domain as {0, 40}; output equivalent weight u, and its variable domain {0, 1}. The quantised factor of the controlled quantity is 0.025. The distance l is as follows:

$$l = \sqrt{(O_i - V_i)^2 + (O_j - V_j)^2} \tag{16}$$

where O_i, O_j represents the abscissa and the ordinate of the observation point respectively. V_i, V_j represents the abscissa and the ordinate of the state update point respectively.

2 Dynamic particle swarm reasoning. The farther the Euclidean distance between the state update point and the observation point, the smaller the equivalent weight. Select the triangular membership function. Table 1 is a specific dynamic PSO rule that corresponds to the input l and output u.

Table 1 The corresponding rules of input and output

l	0~0.5	0.5~1	1~1.5	1.5~2	2~2.5	…	30~40
u	1~0.98	0.98~0.95	0.95~0.92	0.92~0.89	0.89~0.86	…	0

3 The determination of the output equivalent weight u of dynamic PSO. The number of weight u is theoretically dependent on the observation number. According to the control rules, solve the output weight u of the dynamic PSO. From the algorithm synthesis rules, obtain:

$$u = \Delta l \cdot M \tag{17}$$

where u is output equivalent weight for dynamic PSO, Δl is the Euclidean distance between observation point and state update lattice point, M is total dynamic PSO relationship.

4 Solution dynamic PSO for dynamic PSO training output. The output weight u of the dynamic PSO based on the above reasoning is dynamic PSO value and can not be directly applied to the state update equation. It needs to be transformed into an executable precise quantity. This process is generally called the solution dynamic PSO, and the method selected here is the maximum membership degree method.

5 State update process. After the physical space distance obtains the corresponding weight through the dynamic PSO training, each step of the state update variable is obtained by the following formula:

$$x_i^a = x_i^f + \frac{A_{i,:}^f \overset{i}{S}{}^T \left(\overset{i}{S}\overset{i}{S}{}^T\right)^{-1} \left(\overset{i}{y} - \overset{i}{H}{}_x^i f\right) \overset{i}{p}_{i,:} \overset{i}{u}_{i,:}}{\sqrt{N-1}} \tag{18}$$

$$A_{i,:}^a = A_{i,:}^f \left(I + \overset{i}{S}{}^T \overset{i}{S}\right)^{-\frac{1}{2}} \tag{19}$$

where $A_{i,:}$ is the i^{th} line of the set perturbation matrix A; $\overset{i}{y}$ represents local observation data; $\overset{i}{H}$ represents the local observation operator; $\overset{i}{p}_{i,:} \overset{i}{u}_{i,:}$ represents the corresponding weight value for the i position observation; $\overset{i}{S} \equiv \overset{i}{R}{}^{-\frac{1}{2}} \overset{i}{H} \overset{i}{A}{}^f \Big/ \sqrt{N-1}$ represent the local ensemble observation disturbance, which $\overset{i}{R}$ represents local observation error covariance, $\overset{i}{A}$ represents local ensemble perturbation, for updating the state vector of the i^{th} element or the set disturbance matrix of the i^{th} column.

In formulas (3) and (4): let $\overset{i}{K}_{i,:} = A_{i,:}^f \overset{i}{S}{}^T$

$\left(I + \overset{i}{S}\overset{i}{S}{}^T\right)^{-1} \Big/ \sqrt{N-1}, \overset{i}{T} = \left(I + \overset{i}{S}{}^T \overset{i}{S}\right)^{-\frac{1}{2}}, U = \overset{i}{p}_{i,:} \overset{i}{u}_{i,:}$

Collated to get:

$$x_i^a = x_i^f + K_{i,:}^i \left(\overset{i}{y} - \overset{i}{H} \overset{i}{x}{}^f\right) \overset{i}{U} \tag{20}$$

$$A_{i,:}^a = A_{i,:}^f \left(I + \overset{i}{S}{}^T \overset{i}{S}\right)^{-\frac{1}{2}} \tag{21}$$

By updating the variables in each step, we get the background set perturbation. In the assimilation system, we make data fusion and get the analysis mean and covariance matrix in the training range of the dynamic PSO, and then get the state analysis set and the state update value; take the new state estimation as the background value of the next moment, return to the assimilation model, and reciprocate. Figure 4 shows the state update position background error covariance matrix after dynamic PSO training. It can be seen that the new method can reduce the false correlation in the covariance matrix and eliminate the influence of remote observation on the state update.

Figure 4 The influence of dynamic PSO training on covariance matrix, (a) value range of weight (b) background error covariance matrix (c) dependency background error covariance matrix

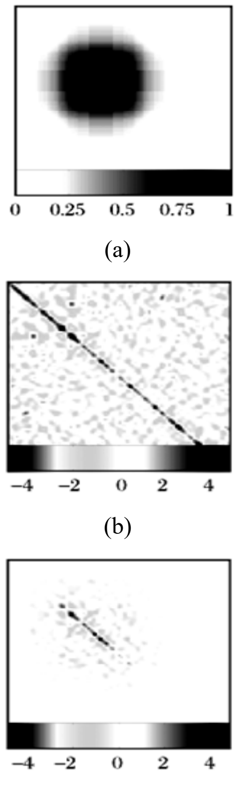

4 Numerical simulation results and analysis

In order to test the performance of the fuzzy control mathematical modelling method based on dynamic PSO training designed in this article, this article conducts the simulation experiment. We use Sphere function and Rastrigin function to carry out fuzzy control and get the consumed time and equilibrium point convergence results of fuzzy control training using particle swarm algorithm in this article, as shown in Figures 5 and 6. It can be seen from the figures that the use of algorithm in this article can effectively reduce the computing overhead, save the running time of the algorithm and improve the fuzzy control.

Figure 5 Training time under different population size

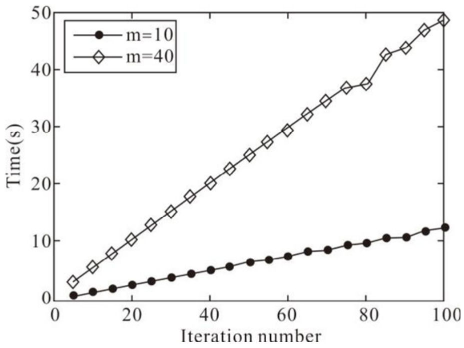

Figure 6 Convergence result of fuzzy control equilibrium point

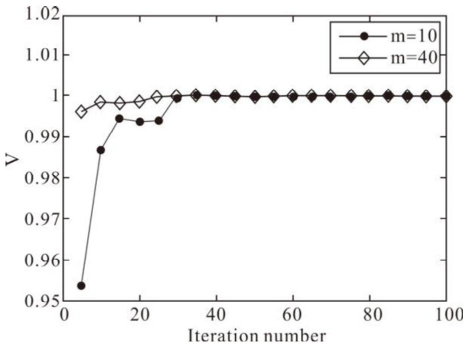

In the experiment, we adopt the root mean square error as the error operator for testing the performance of the assimilation method. The following evaluation indexes are adopted.

$$RMSE_a = \sqrt{\frac{1}{n}\left(\sum_{i=1}^{n}(x-x_i)^2\right)} \tag{22}$$

where n is the dimension of the model state vector, x is the estimated value, x_i is the true value of the model state at t moment.

In order to verify the effectiveness of the fuzzy control ensemble transform Kalman filter (FETKF) in the actual situation, in the experimental model, we discretise the observation position, simulate the randomness and uncertainty of the fixed point observation, and together with ETKF and local ensemble transform Kalman filter (LETKF), compare the set number N, observation number P, model step T, covariance magnifying factor *infl*, chaos model force parameter F, LETKF localisation coefficient, FETKF weight coefficient spce distribution, and observe the influence of parameter changes on different assimilation schemes.

The parameters of the experimental scheme are set as follows: in the experiment 1, the parameters are set as shown in Table 2. Select the set number N change range as [5~50], with an interval of 5. As shown in Figure 7, the root mean square error comparison of the three methods under in different set numbers:

1 With the increase of the set number, the root mean square error of the three methods is gradually decreased, the assimilation accuracy is increased continuously.

2 When the initial set number is 2, the root mean square error of the three methods is large, and it is difficult to meet the requirement of assimilation. With the increase of set number, the convergence speed of FETKF method is the fastest. When the set number is 20, it firstly achieves better assimilation precision. When the set number is 40, the three methods achieve the same assimilation effect.

3 The excessive number of sets will inevitably lead to too much computation burden, while the advantage of the FETKF method compared to the other two methods is the best assimilation effect when the set number is relatively small.

Figure 7 Influence of set number on assimilation results

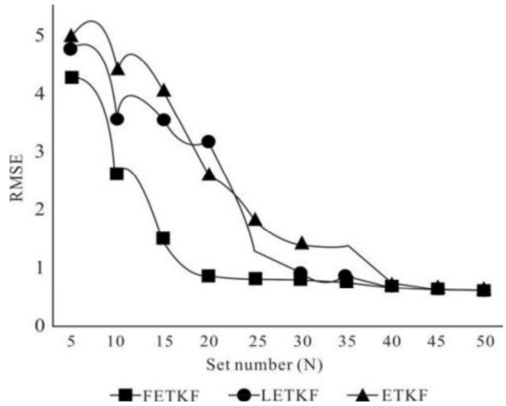

As shown in Figure 8, the root mean square error comparison of three methods under different observation numbers is as follows:

1 With the increase of observation number, the root mean square error of the three methods gradually decreases, and the assimilation accuracy increases.

2 Since the set model is discrete random observation, the ETKF method can not make effective use of the observation data in the assimilation process, resulting in errors, and the effect of assimilation is not ideal. Although the LETKF method only obtains the observation data within the regulated radius range, improves the effectiveness of the observation data, makes the root mean square error less than that of ETKF method, but the LETKF method has too large influence radius, the ensemble number provides limited freedom and has small influence on the analysis value in the assimilation process, even farther observation data on the lattice points with respect to the model resolution is relatively sparse, leading to the observation error covariance matrix estimation error of [20~21]; while if the influence radius is too small, some pattern points can not be influenced by the observed information.

Table 2 Experimental design scheme

	Set number N	*Observation number P*	*Model step length T*	*Magnifying factor infl*	*Force parameter F*
Experiment 1	5~50	10	25	1.01	8
Experiment 2	20	1~20	25	1.01	8
Experiment 3	20	10	5~60	1.01~1.12	8
Experiment 4	20	10	25	1.00	8
Experiment 5	20	10	25	1.01	4~12

3 With the increase of the observation number, the FETKF method can obtain more accurate and effective observation data, which makes the root mean square error minimum and the assimilation precision highest.

4 When the observation is random and uncertain, we can give weight for reasonable observation, get the most reasonable observation information, and eliminate the false correlation between remote observation and state variables.

Figure 8 Influence of observation number on assimilation results

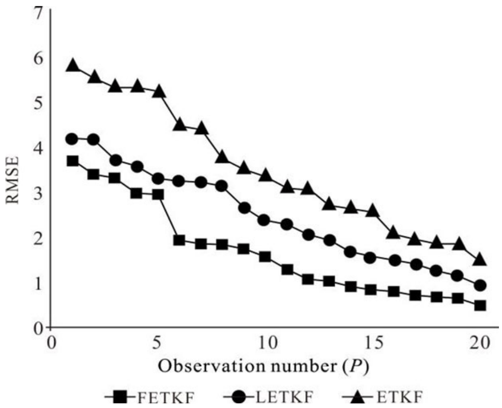

As shown in Figure 9, the comparison of the root mean square error and the comparison of the parameters between the three methods under different force parameters:

1 The larger the force parameter, the more obvious the nonlinearity of the chaotic system. The root mean square error of the ETKF method has been diverged, and the more real state estimation can not be obtained in the chaotic system. The LETKF method and FETKF method, do not have obvious changes of root mean square error with changes of the force parameters. The results show that the two methods have good stability in chaotic system

2 When the force parameter $F = 8$, the root mean square error of both the LETKF method and the FETKF method is the minimum, and the difference between the two kinds of root mean square error is unobvious.

3 When the force parameter $F > 8$, the root mean square error of the LETKF method is obviously greater than that of the FETKF method, so it can be seen that the FETKF method has strong robustness in the chaotic system.

Figure 9 Influence of change of force parametron assimilation results

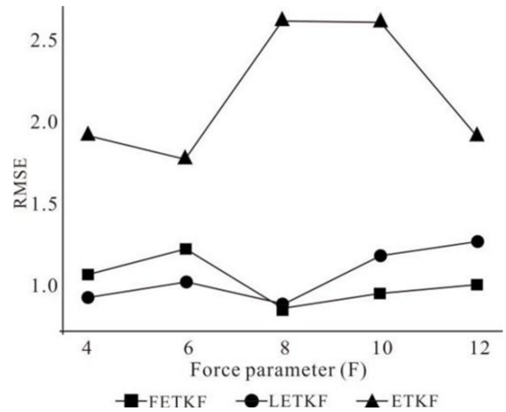

5 Conclusions

In the dynamic PSO training, the optimal state estimation needs constant modification by use of the observation values. This article proposes the fuzzy control mathematical modelling method based on dynamic PSO training. Combined with the ETKF method, it gives the reasonable solution algorithm and calculation process of the nonlinear system. The results show that, under the condition of random and discrete observation, the new method can improve the false correlation of the background error covariance matrix to a certain extent, avoid the influence of the remote observation data on the state update variable, reduce the error caused by difficult use of observation data in the region, reduce the error caused by difficult use of observation data, reduce the computational overhead, and improve the precision of fuzzy control.

Acknowledgements

This work was supported in part by the Mathematical Modeling of Dynamic Particle Swarm Optimisation (Key Projects of Department of Education, Anhui Province on Natural Science Research in Colleges and Universities KJ2016A447); and supported by Innovation and Entrepreneurship Education Model of Higher Vocational Students in the ‘Internet+’ Era (Major Educational Reform Projects of Revitalisation Plan for Higher Education in Anhui Province 2015zdjy180).

References

Chang, X.H. and Yang, G.H. (2010) 'Relaxed stabilization conditions for continuous-time Takagi-Sugeno fuzzy control systems', *Information Sciences*, Vol. 180, No. 17, pp.3273–3287.

Chen, B., Liu, X., Liu, K., Shi, P. and Lin, C. (2010) 'Direct adaptive fuzzy control for nonlinear systems with time-varying delays', *Information Sciences*, Vol. 180, No. 5, pp.776–792.

Crawford, B., Soto, R. and Monfroy, E. (2013) 'Parameter tuning of a choice-function based hyperheuristic using particle swarm optimization', *Expert Systems with Applications*, Vol. 40, No. 5, pp.1690–1695.

Faria, P., Soares, J. and Vale, Z. (2013) 'Modified particle swarm optimization applied to integrated demand response and DG resources scheduling', *IEEE Transactions on Smart Grid*, Vol. 4, No. 1, pp.606–616.

Formisano, M., Turrini, D. and Federico, C. (2013) 'The onset of differentiation and internal evolution: the case of 21 Lutetia', *The Astrophysical Journal*, Vol. 770, No. 1, p.50.

Gandomi, A.H., Yun, G.J. and Yang, X.S. (2013) 'Chaos-enhanced accelerated particle swarm optimization', *Communications in Nonlinear Science and Numerical Simulation*, Vol. 18, No. 2, pp.327–340.

Ghamisi, P., Couceiro, M.S. and Martins, F.M. (2014) 'Multilevel image segmentation based on fractional-order Darwinian particle swarm optimization', *IEEE Transactions on Geoscience and Remote Sensing*, Vol. 52, No. 5, pp.2382–2394.

Helwig, S., Branke, J. and Mostaghim, S. (2013) 'Experimental analysis of bound handling techniques in particle swarm optimization', *IEEE Transactions on Evolutionary Computation*, Vol. 17, No. 2, pp.259–271.

Hu, P., Cao, G.Y., Zhu, X.J. and Hu, M. (2010) 'Coolant circuit modeling and temperature fuzzy control of proton exchange membrane fuel cells', *International Journal of Hydrogen Energy*, Vol. 35, No. 17, pp.9110–9123.

Kalyoncu, M. and Haydim, M. (2009) 'Mathematical modeling and fuzzy logic based position control of an electrohydraulic servosystem with internal leakage', *Mechatronics*, Vol. 19, No. 6, pp.847–858.

Li, D., Zhang, X.H., Yang, D. and Wang, S.L. (2009) 'Fuzzy control of chaos in permanent magnet synchronous motor with parameter uncertainties', *Acta Physica Sinica*, Vol. 58, No. 3, pp.1432–1440.

Lian, K.L., Jhang, J.H. and Tian, I.S. (2014) 'A maximum power point tracking method based on perturb-and-observe combined with particle swarm optimization', *IEEE Journal of Photovoltaics*, Vol. 4, No. 2, pp.626–633.

Lima, N.M.N., Liñan, L.Z., Filho, R.M., Maciel, M.R.W., Embiruçu, M. and Grácio, F. (2010) 'Modeling and predictive control using fuzzy logic: application for a polymerization system', *Aiche Journal*, Vol. 56, No. 4, pp.965–978.

Lin, K.J. (2012) 'Stabilization of uncertain fuzzy control systems via a new descriptor system approach', *Computers & Mathematics with Applications*, Vol. 64, No. 5, pp.1170–1178.

Maldonado, Y., Castillo, O. and Melin, P. (2013) 'Particle swarm optimization of interval type-2 fuzzy systems for FPGA applications', *Applied Soft Computing*, Vol. 13, No. 1, pp.496–508.

Marinakis, Y., Iordanidou, G.R. and Marinaki, M. (2013) 'Particle swarm optimization for the vehicle routing problem with stochastic demands', *Applied Soft Computing*, Vol. 13, No. 4, pp.1693–1704.

Mohammadi-Ivatloo, B., Moradi-Dalvand, M. and Rabiee, A. (2013) 'Combined heat and power economic dispatch problem solution using particle swarm optimization with time varying acceleration coefficients', *Electric Power Systems Research*, Vol. 95, No. 19, pp.9–18.

Mora-Gutiérrez, R.A., Rincón-García, E.A., Ponsich, A., Ramírez-Rodríguez, J. and Méndez-Gurrola, I.I. (2016) 'Influence of social network on method musical composition', *Artificial Intelligence Review*, Vol. 46, No. 2, pp.225–266.

Palafox, L., Noman, N. and Iba, H. (2013) 'Reverse engineering of gene regulatory networks using dissipative particle swarm optimization', *IEEE Transactions on Evolutionary Computation*, Vol. 17, No. 4, pp.577–587.

Roberge, V., Tarbouchi, M. and Labonté, G. (2013) 'Comparison of parallel genetic algorithm and particle swarm optimization for real-time UAV path planning', *IEEE Transactions on Industrial Informatics*, Vol. 9, No. 1, pp.132–141.

Sinha, M., Kuttieri, R.A. and Chatterjee, S. (2013) 'Nonlinear and linear unstable aircraft parameter estimations using neural partial differentiation', *Journal of Guidance, Control, and Dynamics*, Vol. 36, No. 4, pp.1162–1176.

Ting, C.J., Wu, K.C. and Chou, H. (2014) 'Particle swarm optimization algorithm for the Berth allocation problem', *Expert Systems with Applications*, Vol. 41, No. 4, pp.1543–1550.

Vembarasan, V. and Balasubramaniam, P. (2013) 'Chaotic synchronization of Rikitake system based on t-s fuzzy control techniques', *Nonlinear Dynamics*, Vol. 74, Nos. 1–2, pp.31–44.